



# $\Lambda$ and $\Sigma$ Excitations and the Quark Model

E. Klempt<sup>1,2,a</sup>, V. Burkert<sup>2</sup>, U. Thoma<sup>1</sup>, L. Tiator<sup>3</sup>, R. Workman<sup>4</sup>, The Baryon@PDG Group

<sup>1</sup> Helmholtz–Institut für Strahlen–und Kernphysik, Universität Bonn, 53115 Bonn, Germany

<sup>2</sup> Thomas Jefferson National Accelerator Facility, Newport News, VA 23606, USA

<sup>3</sup> Institute of Nuclear Physics, Universität Mainz, 55099 Mainz, Germany

<sup>4</sup> Department of Physics, George Washington University, Washington, DC 20052, USA

Received: 7 July 2020 / Accepted: 19 September 2020 / Published online: 13 October 2020

© The Author(s) 2020

Communicated by Klaus Peters

**Abstract** The spectrum of  $\Lambda$  and  $\Sigma$  excitations is reviewed taking into account (nearly) all hyperon resonances which were seen in early analyses or in one of the recent partial-wave analyses. The spectrum is compared with the old Isgur–Karl model and the Bonn model. These models allow us to discuss the SU(3) structure of the observed resonances. The SU(3) decomposition is compared with SU(6) relations between the different decay modes. Seven  $\Lambda$  states are proposed to be classified as SU(3) singlet states. The hyperon spectrum is compared with the spectrum of  $N$  and  $\Delta$  resonances.

## 1 Introduction

The spectrum of excited states of the nucleon and their internal structure are presently studied in a number of laboratories, experimentally in photo- and electroproduction experiments, at the phenomenological level in partial-wave analyses, and theoretically exploiting the quark model, effective field theories or lattice gauge theory. For recent reviews on baryon spectroscopy, see [1–5]. SU(3) relates the spectrum of nucleon and  $\Delta$  resonances to the hyperon spectrum. In the  $\Lambda$  spectrum, an additional class of resonances turns up that are invariant under the exchange of all three quarks and that belong to the SU(3) singlet. A comparison of the nucleon and hyperon excitation spectra should provide information to what extent SU(3) symmetry holds and may help us in the spectroscopic interpretation of resonances.

Most data on the hyperon spectrum were taken in bubble chambers studying  $K^-$  induced reactions. The hyperon spectrum based on early analyses can be found, e.g., in the 2012 Review of Particle Physics (RPP'2012) [6]. New data in the field of hyperon spectroscopy are scarce. There are

new data from BNL covering the very low-energy region of  $K^- p$  scattering [7–11]. At Jefferson Lab (JLab) the spin and parity of  $\Lambda(1405)$  was determined [12] in a study of the reactions  $\gamma p \rightarrow K^+ \Sigma^\pm \pi^\mp$  and  $\gamma p \rightarrow K^+ \Sigma^0 \pi^0$ . The  $\Lambda(1405)$  line shape was studied with real photons [13] and in electroproduction [14]. A study of the production dynamics of low-mass hyperons was reported in Ref. [15]. Otherwise, no new data were reported since the 1980s. The status remained at a stand-still for a long time.

A first break-through for our understanding of the baryon excitation spectrum was achieved in the work of Isgur and Karl [16,17]. The Isgur–Karl model is based on a non-relativistic Hamiltonian with a confinement potential for the constituent quarks and residual quark–quark interactions via an effective one-gluon exchange; spin–orbit interactions were suppressed. Its relativized version [18] returned similar results. Other quark models followed: Glozman et al. considered the exchange of pseudoscalar mesons between quarks (instead of one-gluon exchange) [19,20]. Hyperons were classified into SU(3) flavor multiplets in Ref. [21]. A relativistic quark–diquark mass operator with direct and exchange interactions was suggested to solve the problem of the *missing resonances* [22–24]. Coulomb-like interactions and a confinement, both expressed in terms of a hyperradius, were suggested to govern the dynamics of quarks in baryons [25]. Faustov and Galkin calculated the hyperon mass spectra in a relativistic quark model [26] in an approximation which assumes that the two light quarks form a diquark. The Bonn model [27–29] is relativistically covariant and based on the Bethe–Salpeter equation with instantaneous two- and three-body forces. The Isgur–Karl and the Bonn model give an expansion of the wave functions into SU(3)-multiplets. We will compare the experimental spectrum with these two models.

Using lattice QCD, the masses of excited baryons that can be formed from  $u$ ,  $d$  and  $s$  quarks have been calculated [30,

<sup>a</sup> e-mail: klempt@hiskp.uni-bonn.de (corresponding author)

31]. The pattern of states is very similar to the one obtained in quark models even though the quantitative agreement is not very convincing. Quark masses were used that correspond to a minimal pion mass just below 400 MeV. The QCD three-quark bound-state problem was used to calculate masses of ground-state baryons and first excitations with  $J^P = 1/2^\pm$  and  $3/2^\pm$  exploiting a generalization of the Faddeev equation by solving the Dyson–Schwinger equation [32,33].

Effective field theories (EFTs), when applied to baryons with  $s$  quarks, concentrated on the role of low-lying resonances in the  $\bar{K}N$   $S$ -wave. Kaiser et al. [34] constructed an effective potential from a chiral Lagrangian, and a resonance emerged as quasi-bound state in the  $\bar{K}N$  and  $\pi\Sigma$  coupled-channel system: the  $\Lambda(1405)1/2^-$  resonance. Oller and Meissner [35] studied the  $S$ -wave  $\bar{K}N$  interaction between the SU(3) octet of pseudoscalar mesons and the SU(3) octet of stable baryons in a relativistic chiral unitary approach with coupled-channels and found two isoscalar resonances below 1450 MeV, at about 1380 MeV and 1434 MeV. The first wider state was interpreted as mainly a singlet, a second state at 1434 MeV as mainly an octet state. A further state at 1680 MeV was also identified as mainly an octet state [36]. The results were confirmed in a number of further studies. A survey of the literature and a discussion of the different approaches can be found in Refs. [37–39].

In spite of the rareness of new data, new analyses have shed new light on the hyperon spectrum. The Kent group (KSU) collected a large set of data on  $K^-p$  interactions at low energies. The partial-wave amplitudes were extracted [40] and fitted using a multichannel parametrization consistent with  $S$ -matrix unitarity [41]. The KSU partial-wave amplitudes were also fitted by the JPAC group in a coupled-channel fit [44]. The JPAC analysis was based on the  $K$ -matrix formalism, with special attention was paid to the analytical properties of the amplitudes and their continuation to the complex angular-momentum plane. The Osaka-ANL group applied a dynamical coupled-channel approach, determined the resonances to achieve a good fit and determined their properties [42,43]. Recently, the Bonn–Gatchina (BnGa) group increased the data set by adding further (old) data and reported the hyperon spectrum [45] and the properties of resonances [46].

## 2 The full spectrum

First, we discuss changes that have been introduced for the next RPP. Up to the 2018 edition, a few resonances were reported that were observed as *bumps* in production experiments without a partial-wave analysis. Their masses were often close to known states. In the  $\Sigma$  sector, there are also several *bumps* that are likely produced by known states. In RPP'2020, the  $\Sigma(1480)$ ,  $\Sigma(1560)$ ,  $\Sigma(1620)$ ,  $\Sigma(1670)$ ,  $\Sigma(1690)$  *bumps* are removed from the tables. The reader

interested in these observations is referred to earlier RPP editions. In the  $\Lambda$  sector, further *bumps* are reported for high masses. These states are claims for new states (even though they are without spin–parity determination) in a mass range not covered by recent partial-wave analyses; they are kept in the tables.

The more recent analyses [41–46] use, to a large extent, the same data as had already been used in the early analyses reported in Ref. [6]. However, the sets of extracted resonances are different. Which ones are right? Consider, e.g.,  $\Sigma$  resonances in the 1850 to 1950 MeV mass region. Early analyses [6] find  $\Sigma(1915)5/2^+$  and  $\Sigma(1910)3/2^-$ <sup>1</sup> as leading resonances and additional evidence for  $\Sigma(1880)1/2^+$  and  $\Sigma(1900)1/2^-$ . The KSU group finds  $\Sigma(1915)5/2^+$ ,  $\Sigma(1900)1/2^-$ , and  $\Sigma(1940)3/2^-$ , the Osaka-ANL group  $\Sigma(1940)1/2^-$ ,  $\Sigma(1890)5/2^+$ , and BnGa finds  $\Sigma(1915)5/2^+$ ,  $\Sigma(1900)1/2^-$ , and  $\Sigma(1910)3/2^-$ . All fits require the leading resonance  $\Sigma(1915)5/2^+$ , only the Osaka-ANL set does not include this state. But for the weaker resonances, there are substantial differences. In the fits, resonances are usually added one by one. If a resonance is added in this mass region, the fit improves when the quantum numbers are appropriate, otherwise the fit does not improve, at least not significantly. However, when more and more resonances are added, the improvement of the fit becomes smaller and smaller. When a good description is reached, no further resonance is added. We assume, e.g., that if in the KSU analysis a  $\Sigma(1910)3/2^-$  would have been tested, instead of  $\Sigma(1940)3/2^+$ , a gain in fit quality would also have been reached. When it is added in addition to  $\Sigma(1940)3/2^+$ , the quality of the fit improves only slightly. No significant improvement is obtained when a  $5/2^-$  resonance is tested: a  $5/2^-$  resonance does not exist in this mass region. Thus both resonances,  $\Sigma(1910)3/2^-$  and  $\Sigma(1940)3/2^+$ , may exist but the data are statistically not sufficient to reveal the existence of the two at the same time. But individually, they may both be uncovered. For these reasons, we consider all observations of a resonance reported in one of the analyses in Refs. [6,41,46], or that were seen in model *A* and *B* in Ref. [43], or that were considered a trustworthy resonance in Ref. [44], as candidates for a true state. In practice, this set mostly coincides with the RPP listings including all resonances with at least one star. In the KSU analysis, the partial-wave amplitudes are constructed in sliced energy bins, and the resonance content in different partial waves seems to be determined independently. However, the energy-independent fit is guided by a first preliminary energy-dependent fit. Table 1 summarizes the list of resonances.

<sup>1</sup> This resonance was formerly called  $\Sigma(1940)3/2^-$ . It was renamed and is now called  $\Sigma(1910)3/2^-$  to avoid to have two  $\Sigma$  resonances with different  $J^P$  but the same mass.

**Table 1**  $\Lambda$  and  $\Sigma$  resonances seen in early analyses [6], by the KSU [41], the Osaka-ANL [43] collaboration, the JPAC [44], and by the BnGa collaboration [46]

$\Lambda(1380) 1/2^-$	$\Sigma(1580) 3/2^-$ [6,44]
$\Lambda(1405) 1/2^-$ [6,41,46]	$\Sigma(1620) 1/2^-$ [6,41,43,44,46]
$\Lambda(1520) 3/2^-$ [6,41,43,44,46]	$\Sigma(1660) 1/2^+$ [6,41,43,44,46]
$\Lambda(1600) 1/2^+$ [6,41,43,44,46]	$\Sigma(1670) 3/2^-$ [6,41,43,44,46]
$\Lambda(1670) 1/2^-$ [6,41,43,46]	$\Sigma(1750) 1/2^-$ [6,41,43,46]
$\Lambda(1690) 3/2^-$ [6,41,43,44,46]	$\Sigma(1775) 5/2^-$ [6,41,43,44,46]
$\Lambda(1710) 1/2^+$ [41]	$\Sigma(1780) 3/2^+$ [6,41]
$\Lambda(1800) 1/2^-$ [6,41,46]	$\Sigma(1880) 1/2^+$ [6,41]
$\Lambda(1810) 1/2^+$ [6,41,43,46]	$\Sigma(1900) 1/2^-$ [6,41,43,46]
$\Lambda(1820) 5/2^+$ [6,41,43,44,46]	$\Sigma(1910) 3/2^-$ [6,46]
$\Lambda(1830) 5/2^-$ [6,41,43,44,46]	$\Sigma(1915) 5/2^+$ [6,41,43,44,46]
$\Lambda(1890) 3/2^+$ [6,41,43,44,46]	$\Sigma(1940) 3/2^+$ [41,44]
$\Lambda(2000) 1/2^-$ [6,41]	$\Sigma(2010) 3/2^-$ [46]
$\Lambda(2050) 3/2^-$ [41,44]	$\Sigma(2030) 7/2^+$ [6,41,43,44,46]
$\Lambda(2070) 3/2^+$ [46]	$\Sigma(2070) 5/2^+$ [6,44]
$\Lambda(2080) 5/2^-$ [43,44,46]	$\Sigma(2080) 3/2^+$ [6,44]
$\Lambda(2085) 7/2^+$ [6,41,43,44]	$\Sigma(2100) 7/2^-$ [6,44,46]
$\Lambda(2100) 7/2^-$ [6,41,44,46]	$\Sigma(2110) 1/2^-$ [41,46]
$\Lambda(2110) 5/2^+$ [6,41,44,46]	$\Sigma(2230) 3/2^+$ [46]
$\Lambda(2325) 3/2^-$ [6]	
$\Lambda(2350) 9/2^+$ [6]	

The JPAC fit [44] described the KSU partial waves [41] reasonably well. However, when observables were calculated from their partial-wave amplitudes, significant discrepancies appeared. For this reason, the JPAC results were not included in the RPP. Here, we include their spectrum of resonances in the discussion (see Figs. 1, 2) except those results that are marked by them as unreliable or as artifacts of the fit.

References [6,41,44,46] assigned the resonances found in their analyses to states listed in the RPP and gave unique values for masses and widths. The Osaka-ANL group [43] reported resonances found in their model *A* or in their model *B* but did not assign them to known states. In Table 1, the Osaka-ANL observations are associated with a known state or listed with a newly proposed name. Some resonances are seen in both Osaka-ANL models, others only in their model *A* or *B*. As Particle Data Group we decided to list in the RPP only resonances which are seen in both model *A* and *B*.

Figure 1 shows the spectrum of all  $\Lambda$  resonances observed in the different analyses. The blocks give the pole masses and the pole widths of resonances. The first (left) entry in each subfigure gives the RPP estimate for mass and width, followed by the KSU result. The results of both, model *A* and *B* from Ref. [43] are shown next. The BnGa and JPAC results are given subsequently. The horizontal lines indicate the resonances and their masses adopted as a final spectrum.

The final entry represents the RPP2020 result. It is given as an educated guess based on a critical judgment of the results from different groups. It is not the statistical mean value of the results and the quoted uncertainties.

The  $\Lambda(1380)1/2^-$  and  $\Lambda(1405)1/2^-$  resonances are below the  $K^-p$  threshold and are not reported in Refs. [41,43,44,46]. When both states exist, only one of them can be interpreted within the quark model. In this paper, we consider  $\Lambda(1405)1/2^-$  as the mainly SU(3) singlet state and  $\Lambda(1380)1/2^-$  as an intruder, a state incompatible with any quark-model interpretation.

There are some cases where all measurements agree within a small band. This holds particularly true for the well-known  $\Lambda(1520)3/2^-$  but also for  $\Lambda(1670)1/2^-$ ,  $\Lambda(1690)3/2^-$ , and  $\Lambda(1815)5/2^+$  that all fall into a narrow mass band. Also very convincing are the observations of  $\Lambda(1890)3/2^+$ ,  $\Lambda(1830)5/2^-$ ,  $\Lambda(2100)7/2^-$ . These resonances are listed with four stars. The results on  $\Lambda(1600)1/2^+$  are also rather consistent; a four-star rating seems appropriate here as well.

$\Lambda(1800)1/2^-$ ,  $\Lambda(1810)1/2^+$ , and  $\Lambda(2110)5/2^+$  are seen in several early studies, and were listed as three-star resonances in [6]). They were confirmed in the KSU, BnGa and partly in the Osaka-ANL (model *B*) analysis. These resonances continue to be listed with three stars.

$\Lambda(2350)9/2^+$  is reported with three stars from early analyses. The recent analyses do not cover this mass range. Therefore, this resonance retains its status.

Under  $\Lambda(2000)$ , the RPP'2012 [6] listed resonance claims near this mass. Two entries under  $\Lambda(2000)$  were reported with  $J^P = 3/2^-$  quantum numbers [47,48] that were considered to be obsolete [6]. They could have been shifted to  $\Lambda(2050)3/2^-$ . The quantum numbers  $J^P = 1/2^-$  stem from Refs. [41,49].

The  $\Lambda(2085)7/2^+$  resonance was seen in [6], and in the KSU, Osaka-ANL, and JPAC analyses. The first mass determination of  $\Lambda(2085)7/2^+$  was 2020 MeV [47] and that mass was used to give the resonance its name. The four later determinations in the RPP found higher masses. The (unweighed) mean value of the five values of Breit–Wigner masses is 2085 MeV; therefore, in this study, we rename this state as  $\Lambda(2085)7/2^+$ .

A  $\Lambda(2080)5/2^-$  was seen in the Osaka/ANL analysis (model *A* and *B*), by JPAC, and by the BnGa group. The Osaka/ANL mass was considerably lower, the JPAC considerably higher in mass compared to the BnGa result. We combined these observations to a single one-star resonance.

The KSU and BnGa reported the states  $\Lambda(1710)1/2^+$  and  $\Lambda(2070)3/2^+$ , respectively. These resonances are not confirmed in other analyses and are listed as one-star resonances.

The Osaka/ANL group reports a  $J^P = 1/2^-$   $\Lambda^*$  resonance at 1512 MeV. It is rather wide; the pole width is 370 MeV. We guess this pole might (mis-)represent the  $\Lambda(1405)1/2^-$  resonance.

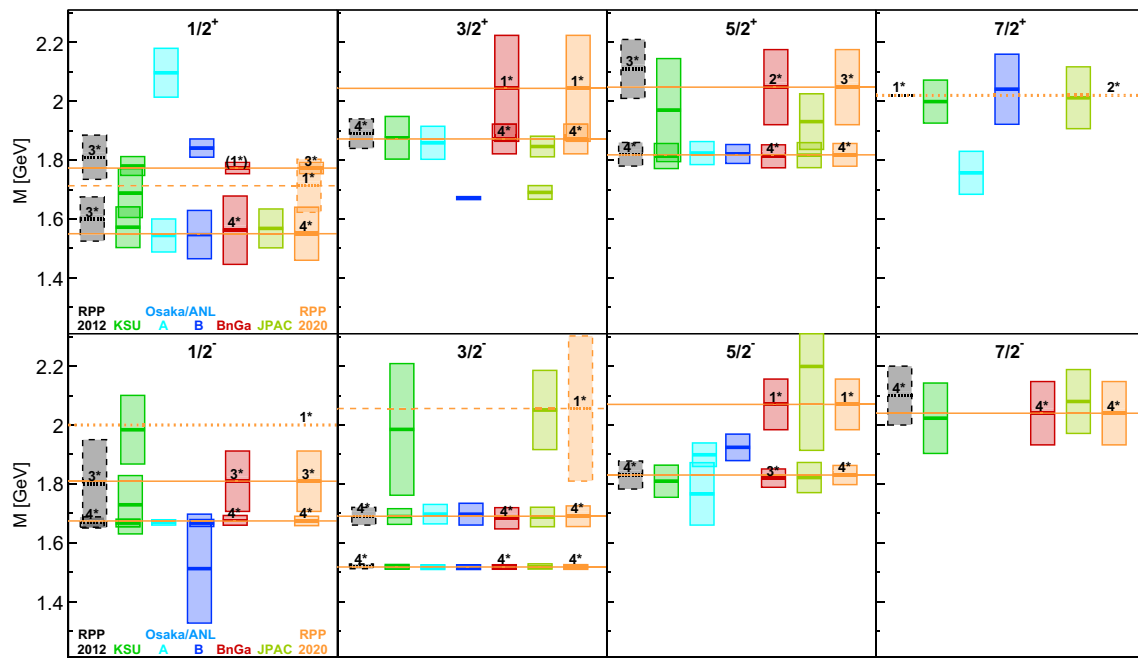


**Fig. 1** Mass spectrum of  $\Lambda^*$  resonances above  $\Lambda(1405)$  for different spin and parities  $J^P$ . For each resonance, the real part of the pole position  $\text{Re}(M_R)$  is given together with a box of length  $\pm \text{Im}(M_R)$ .  $2 \cdot \text{Im}(M_R)$  corresponds to the total width of the resonance. The values of the KSU [41], Osaka/ANL [43], BnGa [45,46], and JPAC [44] analyses are given together with the values given in the RPP'2012 [6] and RPP'2020 listings. Star ratings are indicated for the RPP values and

for the analyses, if available. If no pole positions are given in the RPP (above the line), the RPP Breit–Wigner estimates for masses and widths are used instead. This is indicated by dashed resonance mass lines and dashed lines surrounding the boxes. If an RPP estimate is only available for the resonance mass but not for its width, no box around the respective resonance mass is shown. The RPP'2020 values are extended as lines throughout the picture to allow for better comparison

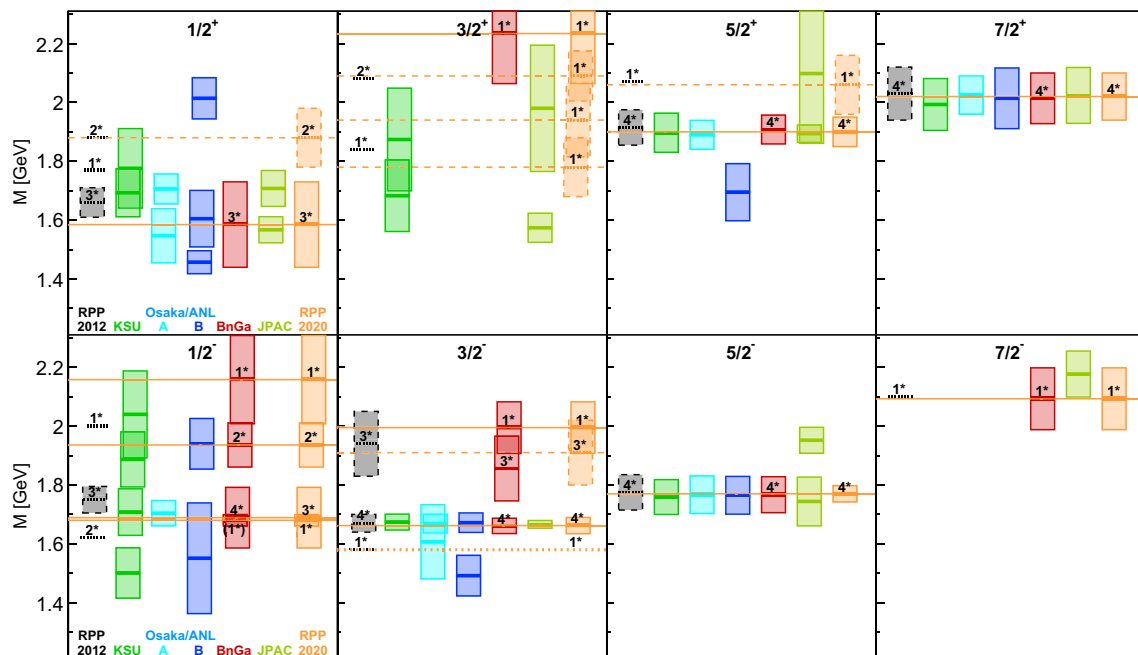


**Fig. 2** Mass spectrum of  $\Sigma^*$  resonances above  $\Sigma(1385)$ . For further explanations, see Fig. 1

**Table 2** Configuration mixing of  $\Lambda$  resonances in the Isgur–Karl [16, 17] (first number) and in Bonn model  $\mathcal{A}$  [27] (second number); the fractions are given in %, n.g. = not given, \* = our value (assuming no mixing with the third excitation band). Shown are negative-parity states in the  $1\hbar\omega$  band and positive-parity states in the  $2\hbar\omega$  band. In

the  $2\hbar\omega$  band, six states with  $J^P = 1/2^+$  are expected, seven with  $J^P = 3/2^+$ , five with  $J^P = 5/2^+$ , and one with  $J^P = 7/2^+$ . The table includes only the lower-mass states; higher-mass states are omitted. The dominant fraction is highlighted

$J^\pi$	Model state	$^28[56]$	$^28[70]$	$^48[70]$	$^28[20]$	$^21[70]$	$^41[20]$	Identified with
$\frac{1}{2}^-$	$[\Lambda \frac{1}{2}^-]_1(1490/1524)$	n.g./2.9	18/26.0	0/0.3	n.g./0.0	<b>81/69.4</b>	n.g./0.2	$\Lambda(1405)1/2^-$
	$[\Lambda \frac{1}{2}^-]_2(1650/1630)$	n.g./5.5	<b>55/61.6</b>	34/2.1	n.g./0.3	15/29.2	n.g./0.1	$\Lambda(1670)1/2^-$
	$[\Lambda \frac{1}{2}^-]_3(1800/1816)$	n.g./0.2	25/3.1	<b>72/94.9</b>	n.g./0.6	3/0.1	n.g./0.6	$\Lambda(1800)1/2^-$
$\frac{3}{2}^-$	$[\Lambda \frac{3}{2}^-]_1(1490/1508)$	n.g./2.0	16/18.7	0.0/0.1	n.g./0.0	<b>83/77.7</b>	n.g./0.1	$\Lambda(1520)3/2^-$
	$[\Lambda \frac{3}{2}^-]_2(1690/1662)$	n.g./4.4	<b>83/72.0</b>	1/2.2	n.g./0.2	16/20.1	n.g./0.0	$\Lambda(1690)3/2^-$
	$[\Lambda \frac{3}{2}^-]_3(1880/1775)$	n.g./0.8	1/1.5	<b>98/96.1</b>	n.g./0.0	0/0.4	n.g./0.4	
$\frac{5}{2}^-$	$[\Lambda \frac{5}{2}^-]_1(1815/1828)$	0*/0.0	0*/0.0	<b>100*/99.0</b>	0*/0.0	0*/0.0	0*/0.4	$\Lambda(1830)5/2^-$
$\frac{1}{2}^+$	$[\Lambda \frac{1}{2}^+]_1(1555/1677)$	<b>99/88.4</b>	0/6.2	0/0.1	0/0.2	1/3.7	0/0.1	$\Lambda(1600)1/2^+$
	$[\Lambda \frac{1}{2}^+]_2(1740/1747)$	1/5.1	9/2.1	0/0.0	0/0.1	<b>90/90.6</b>	0/0.9	$\Lambda(1710)1/2^+$
	$[\Lambda \frac{1}{2}^+]_3(1860/1898)$	0/9.1	<b>83/84.2</b>	8/1.0	0/0.8	8/3.8	0/0.2	$\Lambda(1810)1/2^+$
	$[\Lambda \frac{1}{2}^+]_4(2020/2077)$	0/0.5	8/1.2	<b>72/85.8</b>	19/11.2	1/0.1	1/0.3	
$\frac{3}{2}^+$	$[\Lambda \frac{3}{2}^+]_1(1810/1823)$	<b>62/60.0</b>	24/28.2	1/0.3	0/0.1	12/9.9	1/0.1	$\Lambda(1890)3/2^+$
	$[\Lambda \frac{3}{2}^+]_2(1960/1952)$	1/3.8	8/7.6	31/0.8	0/0.1	<b>47/84.0</b>	11/2.2	$\Lambda(2070)3/2^+$
	$[\Lambda \frac{3}{2}^+]_3(2005/2045)$	12/0.5	0/0.2	<b>60/96.9</b>	1/1.1	20/0.3	9/0.2	
$\frac{5}{2}^+$	$[\Lambda \frac{5}{2}^+]_1(1815/1834)$	<b>65/57.8</b>	23/28.3	0/0.2	0/0.1	12/12.1	0/0.0	$\Lambda(1820)5/2^+$
	$[\Lambda \frac{5}{2}^+]_2(2010/1999)$	2/4.5	18/8.9	0/1.0	0/0.1	<b>79/84.1</b>	1/0.2	$\Lambda(2110)5/2^+$
	$[\Lambda \frac{5}{2}^+]_3(2095, 2078)$	28/9.0	<b>48/9.9</b>	<b>15/77.1</b>	0/0.0	8/2.0	1/0.9	
$\frac{7}{2}^+$	$[\Lambda \frac{7}{2}^+]_1(2070/2130)$	0/0.0	0/0.0	<b>100/99.1</b>	0/0.0	0/0.0	0/0.1	$\Lambda(2085)7/2^+$

Some  $\Sigma$  resonances like  $\Sigma(1670)3/2^-$ ,  $\Sigma(1775)5/2^-$ ,  $\Sigma(1915)5/2^+$ , and  $\Sigma(2030)7/2^+$  are seen with good consistency. They have a four-star status.

The  $\Sigma(1660)1/2^+$  resonance is consistently needed in all analyses. Its Breit–Wigner mass is considerably larger than the pole mass; the pattern resembles the one of the Roper resonance that has a large Breit–Wigner mass and a smaller pole mass. The spread of the values for its mass and width are comparatively large, hence we keep its three-star status.

The  $\Sigma(1620)1/2^-$  resonance was given a two-star status in RPP 2012 [6],  $\Sigma(1750)1/2^-$  was listed with three stars. KSU finds two states. The low-mass pole has a mass of 1501 MeV and a (full) pole width of 171 MeV, the high-mass pole has parameters 1708 MeV and 158 MeV, respectively. Osaka/ANL finds either a low-mass pole (model A) with a substantial width, or (model B) a high-mass pole at  $1764^{+3}_{-6}$  MeV and a full width of  $84^{+14}_{-4}$  MeV (model A). BnGa finds a problematic—and statistically not significant—interference pattern of  $\Sigma(1620)1/2^-$  and  $\Sigma(1750)1/2^-$ . Nevertheless, we keep the three-star status  $\Sigma(1750)1/2^-$  but decided to downgrade  $\Sigma(1620)1/2^-$  to one star.

The  $\Sigma(1880)1/2^+$  resonance was given a two-star status in RPP'2012 [6]. Several other analyses do not confirm this state. Nevertheless, we keep it as two-star resonance.

We exclude the  $\Sigma(1770)1/2^+$  resonance from the Listings. This resonance had been found in a few early analyses. However, the positive result in Ref. [52] was superseded by Ref. [53] where the resonance was found with a mass compatible with  $\Sigma(1660)1/2^+$ . Its observation in Ref. [55] was superseded in Ref. [56], again a mass compatible with  $\Sigma(1660)1/2^+$  was found. The resonance was also reported to exist in Ref. [54], but only one of two solutions required it.

In most cases,  $\Lambda$  and  $\Sigma$  resonances reported only in RPP'2012 [6] or only either in the KSU [41] or in the BnGa [46] analysis are listed as one-star resonances.

The one-star  $\Sigma(1580)3/2^-$  resonance was seen in an analysis of low-statistics data on  $K^-p \rightarrow \pi^0\Lambda$  [50] but has been ruled out by a counter experiment at BNL [9, 51]. It was confirmed in the Osaka/ANL analysis.

The  $\Sigma(1840)3/2^+$  resonance was removed from the Listings. It contains results from early analyses. Two entries are compatible with  $\Sigma(1780)3/2^+$  and one entry is compatible



with  $\Sigma(1940) 3/2^+$ . These entries are moved to the corresponding resonances.

The  $\Sigma(1910)3/2^-$  resonance is a three-star resonance long known as the  $\Sigma(1940)3/2^-$ . Recently, it was confirmed in the BnGa analysis. It was renamed to avoid confusion with  $\Sigma(1940)3/2^+$ .

The  $\Sigma(2000)1/2^-$  resonance has been removed from the listings and the results are transferred to  $\Sigma(1900)1/2^-$ , the mass value derived in Ref. [41]. The resonance was confirmed in the BnGa analysis. The entries are mostly compatible with mass values in the 1900–1950 MeV range.

Resonances reported in none of the three papers [6, 41, 46] or only in Osaka-ANL-model A or B are not taken into account. This holds true, e.g., for  $\Lambda(1687)3/2^+$  and  $\Sigma(1574)3/2^+$  in the JPAC analysis,  $\Lambda(1757)7/2^+$  in Osaka-ANL-model A, and  $\Lambda(2097)7/2^+$ ,  $\Lambda(1671) 3/2^+$ ,  $\Sigma(1695) 5/2^+$  in Osaka-ANL-model B. Furthermore, these states are certainly incompatible with any quark model. They might provide hints for resonances beyond the quark model, or they could be artifacts of the fit. We disregard them in the further evaluations.

The discussion of the various observed states and the large uncertainties demonstrate the need for new data. Prospects will be discussed at the end of the paper.

### 3 Symmetry considerations

In the quark model, the wave function of a baryon contains three constituent quarks. The wave function is the product of four parts describing the spatial, spin, flavor, and color configuration. The Pauli principle requires the baryon to be antisymmetric with respect to the exchange of any pair of quarks. Confinement requires the color wave function to be antisymmetric, hence the spatial-spin-flavor wave function needs to be symmetric.

For baryons with light-quark flavors (i.e. up, down, and strange ( $u$ ,  $d$ ,  $s$ ) quarks) only, the baryon flavor wave function can be decomposed into a decuplet which is symmetric with respect to the exchange of any two quarks, a singlet which is antisymmetric and two octets of mixed symmetry. The latter can be further classified into a mixed symmetric and a mixed antisymmetric representation:

$$3 \otimes 3 \otimes 3 = 10_S \oplus 8_M \oplus 8_M \oplus 1_A. \quad (1)$$

$\Lambda$  hyperons can be in the flavor SU(3) singlet or octet,  $\Sigma$  hyperons in the SU(3) octet or decuplet.

The spin wave function can be classified according to SU(2) representations, the spin-flavor wave function can be classified according to  $SU(2) \otimes SU(3) = SU(6)$  representations:

$$6 \otimes 6 \otimes 6 = 56_S \oplus 70_M \oplus 70_M \oplus 20_A. \quad (2)$$

The states in each of these representations can be decomposed according to  $SU(2) \otimes SU(3)$ ,

$$56 = {}^4 10 \oplus {}^2 8. \quad (3)$$

i.e. into a flavor symmetric decuplet combined with a spin symmetric quartet and the symmetric combination of mixed symmetric flavor octet and mixed symmetric spin-doublet states. This spin-flavor wave function can be combined with a symmetric spatial-wave function.

The mixed symmetric 70-plet can be decomposed as

$$70 = {}^2 10 \oplus {}^4 8 \oplus {}^2 8 \oplus {}^2 1. \quad (4)$$

It needs to be combined with a spatial-wave function of mixed symmetry. A ground state has a symmetric spatial-wave function, hence SU(3) singlet  $\Lambda$  states always carry an orbital or radial excitation.

Finally, the antisymmetric 20-plet contains the antisymmetric combination of a flavor mixed symmetric octet with a mixed symmetric spin doublet and the antisymmetric flavor singlet combined with a symmetric spin quartet:

$$20 = {}^2 8 \oplus {}^4 1. \quad (5)$$

Nucleon and  $\Delta$  resonances are easily identified:  $\Delta$  exist in the four charge states  $\Delta^-$ ,  $\Delta^0$ ,  $\Delta^+$ ,  $\Delta^{++}$ ; nucleons only in two charge states. Their decays are governed by the well-conserved isospin symmetry.  $\Lambda$  resonances in SU(3) singlets or octets are always neutral in charge,  $\Sigma$  resonances in octets or decuplets are found in three charge states. A classification according to their SU(3) structure suffers from two aspects:  $\Lambda$  resonances in SU(3) singlet or octet configurations—or  $\Sigma$  resonances in SU(3) octet or decuplet configurations—can mix; second, SU(3) symmetry is significantly broken.

### 4 Configuration mixing of $\Lambda$ resonances

#### 4.1 Comparison with quark models

The resulting spectrum is now compared to the classical Isgur-Karl model [16, 17] and the later Bonn model [27]. We do not compare the experimental spectrum with lattice results [30, 31] or quark-model calculations [63, 64] that did not provide their results in numerical form. These calculations also do not give quantitative results on the mixing of singlet and octet  $\Lambda$  or octet and decuplet  $\Sigma$  states.

In Table 2,  $\Lambda$  resonances in the first and second excitation band are listed in each partial wave by assuming that all resonances have been seen up to a maximum mass. Not all resonances in the second band are listed; entries with high mass values for which no experimental candidates exist are not included in Table 2 (nor in Table 5). In particular, resonances belonging to the 20-plet are all missing. The configuration of resonances in the third band and in higher bands is not given

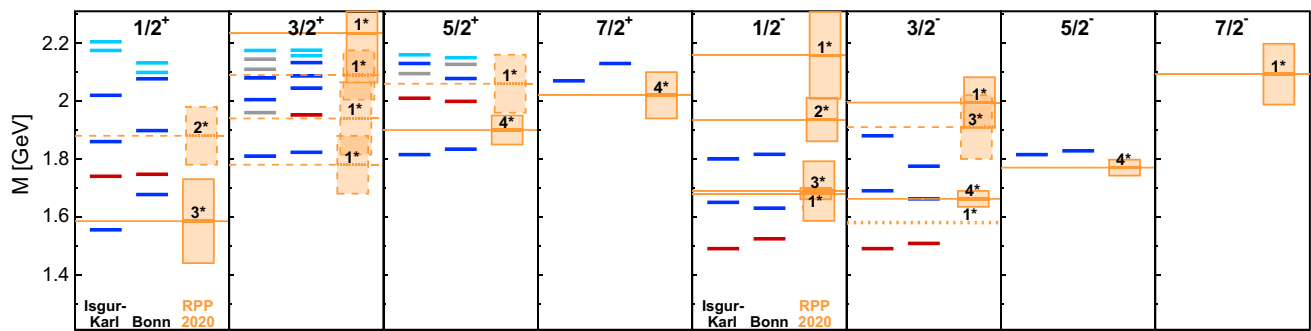


**Fig. 3**  $\Lambda^*$  states given in the RPP'2020 are compared to the quark-model states of the  $1\hbar\omega$  and  $2\hbar\omega$  band calculated by Isgur–Karl [16, 17] and within the Bonn model [27]. For explanations related to the RPP-states, see Fig. 1. For the quark-model states, the colors indicate the

main configuration of the state, if one specific configuration reaches a value above 50%:  $2^1[70]$  (red),  $2^8[56]2^8[70]$  or  $4^8[70]$  (blue),  $2^8[20]4^1[20]$  (cyan), strong mixing, none of the configuration reaches 50% (gray). The experimental results for  $\Lambda(1405)1/2^-$  are given in the text only

in the publications. The comparison of experimental masses with predicted masses is visualized in Fig. 3.

Some  $\Lambda$  resonances with a given spin–parity  $J^P$  may have contributions from quark-spin doublets or quark-spin quartets, they may have a symmetric or antisymmetric spatial-wave function or a wave function with mixed symmetry. They can be in a flavor singlet or octet state. These internal quantum numbers are not observable, hence all these configurations can mix when they have the same spin–parity. Table 2 gives the probability that a physical state with defined  $J^P$  has a given set of internal quantum numbers. Reference [27] uses a fully relativistic treatment and a small fraction of the wave function is found at negative energy; these fractions are omitted here. In Refs. [16, 17], amplitudes are given from which we calculated the probabilities. In Ref. [27], the two configurations  $4^8[70]$  with intrinsic  $S$ -wave or  $D$ -wave orbital excitation are not given separately. To allow for an easier comparison, the two contributions calculated in Ref. [17] are added.

Given the large differences in the model assumptions, the agreement between the two models is remarkable. In particular, the largest contributions, underlined in Table 2, are mostly the same in both calculations. In the negative-parity sector, the doublet  $\Lambda(1405)1/2^-$  and  $\Lambda(1520)3/2^-$  have a large fraction in the  $2^1[70]$  configuration,  $\Lambda(1670)1/2^-$  and  $\Lambda(1690)3/2^-$  are dominantly  $2^8[70]$ , and  $\Lambda(1800)1/2^-$  and  $\Lambda(1830)5/2^-$  belong to a spin-quartet  $4^8[70]$  (degenerated to a triplet) where the  $3/2^-$  state is missing. The octet  $\Lambda$  resonances have all analogue states in the nucleon sector about 100–150 MeV lower in mass.

In the positive-parity sector, the  $\Lambda(1600)1/2^+$  resonance plays the role of the Roper  $N(1440)1/2^+$ ,  $\Lambda(1810)1/2^+$  the role of  $N(1710)1/2^+$ . Between these two states, there is a further state,  $\Lambda(1710)1/2^+$ , which cannot be mapped onto the nucleon spectrum and is interpreted as an SU(3) singlet state in both quark models.

The two resonances  $\Lambda(1890)3/2^+$  and  $\Lambda(1820)5/2^+$  can be assigned to states that belong—with a  $\approx 60\%$  probability—to a  $2^8$  configuration in the 56-plet;  $N(1720)3/2^+$  and  $N(1680)5/2^+$  are their partners in the nucleon sector.

The  $\Lambda(2085)7/2^+$  resonance is a bit low in mass when compared to  $N(1990)7/2^+$ ; however, their spectroscopic identification is unique: both resonances must belong to the  $4^8[70]$ -plet.

A slight discrepancy between the Isgur–Karl and the Bonn model in the spectroscopic assignment is found for the  $\Lambda(2070)3/2^+$  resonance. In the Bonn model, this state is predominantly a singlet state, in the  $2^1[70]$ -plet. In the Isgur–Karl model, it is strongly mixed even though the  $2^1[70]$ -plet configuration prevails. The lattice results [31] see the first state above  $\Lambda(1890)3/2^+$  as singlet state.  $\Lambda(2110)5/2^+$  seems to be the spin partner of  $\Lambda(2070)3/2^+$ . The next-higher state with  $J^P = 5/2^+$  is predicted at 2095 or 2078 MeV, depending on the model, it could be in a spin doublet or spin quartet.

## 4.2 SU(3) constraints for $\Lambda^*$ decays

The decays of hyperons are governed by the available phase space, the angular-momentum barrier, and by symmetric ( $d_{ijk}$ ) and antisymmetric ( $f_{ijk}$ ) SU(3) structure constants. These are tabulated, e.g., in the RPP. Their relative contribution is governed by the so-called  $F/D$  ratio that is usually parameterized as  $F/D = \alpha/(1 - \alpha)$ . In SU(3),  $\alpha$  is a free parameter but within SU(6),  $\alpha$  can be predicted. With the values for  $\alpha$  given in Table 3, the SU(6) coupling constants can be calculated (see, e.g., [59, 60]). The corresponding coupling constants are listed in Table 3. The initial state cancels in the comparison, and the relative sign of the amplitudes can be used to determine the SU(3) structure of a hyperon.

The ratios of the decay amplitude for decays of  $\Lambda$  resonances into  $N\bar{K}$  and  $\Sigma\pi$ , derived from SU(3) relations and

**Table 3** SU(3) coupling constants for hyperon decays and the SU(6) predictions for the coefficient  $\alpha$  in decays of octet hyperons

Decay mode	$8 \rightarrow 8 + 8$		$1 \rightarrow 8 + 8$	
$\Lambda \rightarrow N \bar{K}$	$\sqrt{\frac{2}{3}}(2\alpha + 1)A_8$		$\frac{1}{2}A_1$	
$\Lambda \rightarrow \Sigma \pi$	$2(\alpha - 1)A_8$		$\sqrt{\frac{3}{2}}A_1$	
	${}^2_8[56]$		${}^2_8[70]$	
$\alpha$	$\frac{2}{5}$		$\frac{5}{8}$	
	${}^2_1[70]$		${}^2_8[70]$	
	${}^2_1[70]$		${}^2_8[70]$	
$\frac{A(\Lambda \rightarrow N \bar{K})}{A(\Lambda \rightarrow \Sigma \pi)}$	$\sqrt{\frac{1}{6}}$		$-\sqrt{\frac{3}{2}}$	
Sign	+		-	

imposing constraints from SU(6), cannot be expected to be fulfilled. This can best be seen in heavy-quark baryons. In  $\Xi_b$ , the  $u$  and the  $s$  quark are antisymmetric with respect to their exchange, in  $\Xi'_b$ , the  $u$  and  $b$  quark are antisymmetric. The mass difference between the two states is 110 MeV. A potential "SU(3) symmetry in the  $u, s, b$ -quark sector" is heavily broken, a better basis is the flavor  $u, s, b$ -quark basis. This limit is called "ideal mixing for baryons". Likewise, the SU(3) symmetry is broken in the  $u, d, s$ -quark sector and possibly, the physical states do not respect a symmetry in which  $u, d, s$  quarks can arbitrarily be exchanged but are better described in a  $u, d, s$  basis. Thus, we cannot expect branching ratios to respect SU(6) symmetry. Experimentally, however, the relative sign of the amplitude often signals the singlet or octet status of a  $\Lambda$  resonance. Hence we discuss here only the relative sign of the amplitudes for  $K^- p \rightarrow \Lambda^* \rightarrow N \bar{K}$  and  $K^- p \rightarrow \Lambda^* \rightarrow \Sigma \pi$ .

Table 4 lists the phases given in Refs. [41, 43] and [46]. The results are organized into three blocks, one in which phases are given for resonances that are—based on Table 2—supposed to be SU(3) singlets, the second one contains resonances supposed to be in SU(3) octets. The third block lists octet resonances assigned to the  ${}^4[70]$ -plet where the SU(6) phase is not defined. Rescattering in the final state and background contributions can lead to a shift of the phase; we interpret values which are compatible the range  $-35^\circ < \delta < 35^\circ$  as consistent with  $\delta = 0^\circ$  and the range  $145^\circ < \delta < 215^\circ$  as consistent with  $\delta = 180^\circ$ .

The singlet candidates have mostly phases which are compatible with this assignment. The phase difference of the amplitude for  $K^- p \rightarrow \Lambda(1520)3/2^- \rightarrow \bar{K} N$  and  $\rightarrow \Sigma \pi$  is  $\delta = 0^\circ$  in the KSU analysis. Osaka-ANL and BnGa determined the phase difference of the normalized residues at the pole position and found  $\delta = 1^\circ$  or  $\delta = (5 \pm 4)^\circ$ , respectively, compatible with  $0^\circ$ . Hence  $\Lambda(1520)3/2^-$  is dominantly an SU(3) singlet state. The two states  $\Lambda(2080)5/2^-$  and  $\Lambda(2100)7/2^-$  belong to the third excitation band and

**Table 4** The phase difference  $\delta\phi$  between the amplitudes for  $K^- p \rightarrow \Lambda^* \rightarrow \Sigma \pi$  and  $K^- p \rightarrow \Lambda^* \rightarrow K^- p$  on the real axis (2012, KSU) and at the  $\Lambda^*$  pole (Osaka-ANL and BnGa). 2012 stands for results listed in Ref. [6]; in the case of inconsistent results, the signs reported more often are given here. The relative sign or phase is not given in Ref. [44]. For the Osaka-ANL (OA), the results from model A and B are quoted. A – sign indicates that the resonance was not reported. Resonances belonging to a spin quartet are predicted not to couple to  $\bar{K} N$  when they do not mix with other configurations. See text for which phases are to be "expected"

$\Lambda^*$	Expected: $\delta\phi = 0^\circ$				
	2012	KSU	OA <sub>A</sub>	OA <sub>B</sub>	BnGa
$\Lambda(1520)3/2^-$	–	$0^\circ$	$1^\circ$	$1^\circ$	$-(5 \pm 4)^\circ$
$\Lambda(1710)1/2^+$	–	$180^\circ$	–	–	–
$\Lambda(2070)3/2^+$	–	–	–	–	$-(10 \pm 13)^\circ$
$\Lambda(2080)5/2^-$	–	–	–	–	$(46 \pm 22)^\circ$
$\Lambda(2100)7/2^-$	$0^\circ$	$0^\circ \dagger$	–	–	$(5 \pm 18)^\circ$
$\Lambda(2110)5/2^+$	$0^\circ$	$0^\circ$	–	–	$-(5 \pm 21)^\circ$
$\Lambda^*$	Expected: $\delta\phi = \pm 180^\circ$				
	2012	KSU	OA <sub>A</sub>	OA <sub>B</sub>	BnGa
$\Lambda(1600)1/2^+$	$180^\circ$	$180^\circ$	$-172^\circ$	$-139^\circ$	$-(149 \pm 14)^\circ$
$\Lambda(1670)1/2^-$	$180^\circ$	$180^\circ$	$-39^\circ$	$-29^\circ$	$-(70 \pm 18)^\circ$
$\Lambda(1690)3/2^-$	$180^\circ$	$180^\circ$	$-176^\circ$	$-174^\circ$	$-(157 \pm 8)^\circ$
$\Lambda(1810)1/2^+$	$180^\circ$	$180^\circ$	–	$40^\circ$	$(152 \pm 35)^\circ$
$\Lambda(1820)5/2^+$	$180^\circ$	$180^\circ$	$-179^\circ$	$-177^\circ$	$-(164 \pm 7)^\circ$
$\Lambda(1890)3/2^+$	$180^\circ$	$180^\circ$	$127^\circ$	–	$(148 \pm 16)^\circ$
$\Lambda(2000)1/2^-$	$180^\circ$	$180^\circ$	–	–	–
$\Lambda(2050)3/2^-$	$180^\circ$	$0^\circ$	–	–	–
$\Lambda^*$	Undefined				
	2012	KSU	OA <sub>A</sub>	OA <sub>B</sub>	BnGa
$\Lambda(1800)1/2^-$	$180^\circ$	$180^\circ$	–	–	$(134 \pm 11)^\circ$
$\Lambda(1830)5/2^-$	$180^\circ$	$180^\circ$	$-101^\circ$	$2^\circ$	$(160 \pm 17)^\circ$
$\Lambda(2085)7/2^+$	$180^\circ$	$0^\circ$	–	$2^\circ$	–

are not listed in Table 4. They are assumed to belong to the SU(3) singlet series because of their decays (see below).

A mismatch is  $\Lambda(1710)1/2^+$ . Based on the KSU analysis, it should be a SU(3) octet state, based on Table 2 the assignment to the SU(3) singlet series is preferred. It is neither seen in any of the early analyses nor by Osaka-ANL nor by BnGa; obviously it is difficult to extract from the data. Thus we believe it to be a SU(3) singlet state even though the KSU analysis favors it as SU(3) octet state.

For the octet candidates, the early analyses and Kent find mostly phases that are compatible with the octet interpretation, except for the Kent result on  $\Lambda(2050)3/2^-$ . For  $\Lambda(1670)1/2^-$  Osaka-ANL finds, instead of the expected  $180^\circ$ , a value at about  $-34^\circ$ , BnGa finds  $\delta = (-70 \pm 18)^\circ$ .



This is a clear unresolved discrepancy. For  $\Lambda(1810)1/2^+$ , only Osaka/ANL deviates from the expectation.

$\Lambda(2000)1/2^-$  and  $\Lambda(2050)3/2^-$  are not listed in Table 2. About 150 MeV below their masses, there is a  $N(1875)3/2^-$ . It is accompanied by  $N(1895)1/2^-$  and not by a  $5/2^-$  state. Hence these two  $N^*$  states form a spin doublet. Since there is a spin triplet (a degenerate spin quartet) of negative-parity  $\Delta$  states close by (at 1900, 1940, 1930 MeV with  $J^P = 1/2^-, 3/2^-, 5/2^-$ ), we assign these three  $\Delta$  and the two nucleon resonances to a [56]-plet with a  $^410$  quartet and a  $^28$  doublet.  $\Lambda(2000)1/2^-$  and  $\Lambda(2050)3/2^-$  may form a spin doublet and could be the hyperon partners of the two  $N^*$  states. Indeed,  $\Lambda(2000)1/2^-$  is identified in the early analyses and by Kent—via its phases—as an octet state. The results on  $\Lambda(2050)3/2^-$  are ambiguous.

Finally, we discuss the three states  $\Lambda(2070)3/2^+$ ,  $\Lambda(2110)5/2^+$ , and  $\Lambda(2085)7/2^+$ . At the first glance, they seem to belong to a spin-quartet  $^48[70]$ -plet in the second excitation band. For  $\Lambda(2085)7/2^+$ , there is no alternative interpretation. For quartet states, no phase can be predicted on the basis of SU(6). The Bonn model suggests that the other two states could belong to the singlet series. This is confirmed by the BnGa phases.

#### 4.3 $\Lambda(1380)1/2^-$ and $\Lambda(1405)1/2^-$

In this section, we interpret the  $\Lambda(1405)1/2^-$  and the  $\Lambda(1520)3/2^-$  resonances as  $qqq$  resonances in which one of the quarks is excited to the  $p$  state. However, this interpretation is not uncontested. In modern approaches based on effective field theories, the  $\Lambda(1405)1/2^-$  resonance emerges as quasi-bound state in the  $\bar{K}N$  and  $\pi\Sigma$  coupled-channel system and an additional state, named  $\Lambda(1380)1/2^-$ , appears in RPP'2020. The two states are *dynamically generate*; see Refs. [37, 38]. In a recent paper, Meißner suggested that a hadron resonance may manifest itself as a two-pole structure [39].

Decades ago, the quark model predicted the existence of states like  $N(1440)1/2^+$ ,  $N(1535)1/2^-$ ,  $\Delta(1700)3/2^-$ . These states have more recently also been interpreted as dynamically generated resonances (see [66–69] and the references therein). Analyses of CLAS results on electroexcitation amplitudes demonstrated that the structure of  $N(1440)1/2^+$  and  $N(1535)1/2^-$  cannot be understood as singularities in the meson–baryon scattering amplitudes or as only dynamically generated resonances; the three-quark core needs to be taken into account [70].

The quark model requires one low-mass  $\Lambda$  resonance with  $J^P = 1/2^-$  that is dominantly an SU(3) singlet state. Models based on effective field theories assign a large SU(3) singlet component to  $\Lambda(1380)1/2^-$ . In any case, one and only one of the two states  $\Lambda(1380)1/2^-$  and  $\Lambda(1405)1/2^-$  can and has to be assigned to the predicted quark-model

state. The other one—if it exists—must be an extra state, an intruder, incompatible with any quark-model interpretation. The authors of Ref. [71] extrapolate the Regge trajectory of  $\Lambda(2020)7/2^+$ ,  $\Lambda(1830)5/2^-$ , and  $\Lambda(xxx)3/2^+$  and claim that  $\Lambda(1405)1/2^-$  mostly likely belongs to a leading trajectory of three-quark states. The additional state,  $\Lambda(1380)$ , is suggested to be a pentaquark or a molecular state. Of course, it is debatable if the expected SU(3) singlet state should share a Regge trajectory with SU(3) octet states.

## 5 Configuration mixing of $\Sigma$ resonances

### 5.1 Comparison with quark models

Table 5 compares the experimental  $\Sigma$  excitation spectrum in the first and second excitation band with the Isgur–Karl [16, 17] and the Bonn model [27]. Again, not all resonances in the second band are listed. The configuration of resonances in the third band and in higher bands is not given in the publications. The comparison of experimental masses with predicted masses is visualized in Fig. 4.

$\Sigma$  resonances with a given spin–parity  $J^P$  can be mixtures of different SU(6)⊗O(3) eigenstates; they may have a symmetric or antisymmetric spatial-wave function or a wave function with mixed symmetry.  $\Sigma$  resonances can be in a flavor octet or decuplet state. For some spin–parities, they can be in a quark-spin doublet or quark-spin quartet. Table 5 gives the probability that a physical state with defined  $J^P$  has a given set of internal quantum numbers. In Ref. [27], the two configurations  $^48[70]$  and  $^48[56]$  are not given separately and their contributions given in [17] are added.

In most cases, there is reasonably good agreement between the quark model calculations and the experimental masses. Mostly, the largest contributions, underlined in Table 2, are the same in both calculations. However, there are a few exceptions.

In the first  $\Sigma$  excitation band, we expect three states with  $J^P = 1/2^-$  and  $J^P = 3/2^-$  and one state with  $J^P = 5/2^-$ ; see Table 5. The states in flavor octet and with total quark spin 1/2 as dominant configuration are lower in mass; their flavor and their spin wave functions are in a mixed symmetry configuration. One pair of quarks is antisymmetric in spin and flavor, this is often called a *good diquark*.

The other states are predicted to be close in mass. Expected are a triplet of states with  $J^P = 1/2^-, 3/2^-, 5/2^-$  in the SU(3) octet, and a doublet of states  $J^P = 1/2^-, 3/2^-$  in the SU(3) decuplet. These are of mixed symmetry in flavor and symmetric in the spin configuration, or symmetric in flavor and of mixed symmetry in spin. These wave functions do not contain a good diquark. The mass sequence of the two upper  $J^P = 3/2^-$  is reversed in the two models: In the Isgur–Karl model, the two states are very close, separated by

**Table 5** Configuration mixing of  $\Sigma$  resonances in the Isgur–Karl (first number) and in Bonn model  $\mathcal{A}$  (second number); the fractions are given in %, n.g. = not given, \* = our value (assuming no mixing with the third excitation band). Shown are negative-parity states in the  $1\hbar\omega$  band and positive-parity states in the  $2\hbar\omega$  band. The two states with a dagger

† have two possible assignments, they may belong to the first or to the third (not shown) excitation band. In the  $2\hbar\omega$  band, six states with  $J^P = 1/2^+$  are expected, eight with  $J^P = 3/2^+$ , five with  $J^P = 5/2^+$ , and two with  $J^P = 7/2^+$ . Higher-mass states are omitted

$J^\pi$	Model state	$^28[56]$	$^28[70]$	$^48[70]$	$^28[20]$	$^410[56]$	$^210[70]$	Identified with
$1^-$	$[\Sigma \frac{1}{2}^-]_1(1650/1628)$	n.g./5.4	<b>67/87.4</b>	29/2.3	n.g./0.1	n.g./0.0	3/3.4	$\Sigma(1620)1/2^-$
	$[\Sigma \frac{1}{2}^-]_2(1750/1771)$	n.g./0.2	21/2.9	<b>66/94.6</b>	n.g./0.2	n.g./0.3	12/1.1	$\Sigma(1750)1/2^-$
	$[\Sigma \frac{1}{2}^-]_3(1810/1798)$	n.g./0.1	11/2.8	4/1.7	n.g./0.3	n.g./0.0	<b>85/94.4</b>	$\Sigma(1900)1/2^-$ †
$3^-$	$[\Sigma \frac{3}{2}^-]_1(1675/1669)$	n.g./5.1	<b>92/89.0</b>	1/1.2	n.g./0.1	n.g./0.0	7/3.4	$\Sigma(1670)3/2^-$
	$[\Sigma \frac{3}{2}^-]_2(1805/1728)$	0*/0.1	2*/0.1	41*/ <b>82.7</b>	0*/0.1	0*/0.2	<b>57*/16.0</b>	–
	$[\Sigma \frac{3}{2}^-]_3(1815/1781)$	n.g./0.2	6/4.4	<b>58/15.0</b>	n.g./0.2	n.g./0.0	<b>36/79.3</b>	$\Sigma(1910)3/2^-$ †
$5^-$	$[\Sigma \frac{5}{2}^-]_1(1760/1770)$	0*/0.0	0*/0.0	<b>100*/99.0</b>	0*/0.0	0*/0.2	0*/0.0	$\Sigma(1775)5/2^-$
	$[\Sigma \frac{1}{2}^+]_2(1640/1760)$	<b>94/96.1</b>	5/2.3	0/0.0	0/0.1	0/0.0	1/0.2	$\Sigma(1660)1/2^+$
	$[\Sigma \frac{1}{2}^+]_3(1910/1947)$	4/6.9	<b>82/88.4</b>	9/0.9	0/0.3	1/0.0	3/2.5	$\Sigma(1880)1/2^+$
$3^+$	$[\Sigma \frac{1}{2}^+]_4(1995/2009)$	1/0.0	7/0.2	18/8.4	1/0.1	<b>67/89.9</b>	6/0.4	
	$[\Sigma \frac{1}{2}^+]_5(2025/2052)$	1/0.8	0/1.8	15/1.2	2/1.9	0/0.2	<b>82/93.2</b>	
	$[\Sigma \frac{3}{2}^+]_1(1865/1896)$	0/ <b>73.9</b>	0/22.2	8/0.6	0/0.1	<b>91/0.0</b>	0/2.0	$\Sigma(1780)3/2^+$
$5^+$	$[\Sigma \frac{3}{2}^+]_2(1935/1961)$	<b>86/0.0</b>	8/0.0	2/5.1	0/0.1	<b>1/93.9</b>	3/0.1	$\Sigma(1940)3/2^+$
	$[\Sigma \frac{3}{2}^+]_3(2005/2011)$	2/1.5	10/1.5	41/17.3	1/1.4	<b>43/73.4</b>	2/4.0	$\Sigma(2080)3/2^+$
	$[\Sigma \frac{5}{2}^+]_1(1940/1956)$	<b>88/77.8</b>	7/18.2	0/0.2	0/0.0	0/0.0	4/2.5	$\Sigma(1915)5/2^+$
$7^+$	$[\Sigma \frac{5}{2}^+]_2(2035/2027)$	0/2.9	4/7.8	19/16.3	0/0.0	<b>77/65.9</b>	1/6.0	$\Sigma(2070)5/2^+$
	$[\Sigma \frac{5}{2}^+]_3(2060/2071)$	7/14.0	<b>88/72.0</b>	0/7.6	0/0.0	4/4.9	0/0.4	
	$[\Sigma \frac{7}{2}^+]_1(2015/2070)$	0/0.0	0/0.0	24/29.4	0/0.0	<b>76/69.6</b>	0/0.0	$\Sigma(2030)7/2^+$
	$[\Sigma \frac{7}{2}^+]_2(2115/2161)$	0/0.0	0/0.0	<b>76/70.0</b>	0/0.0	24/29.2	0/0.0	

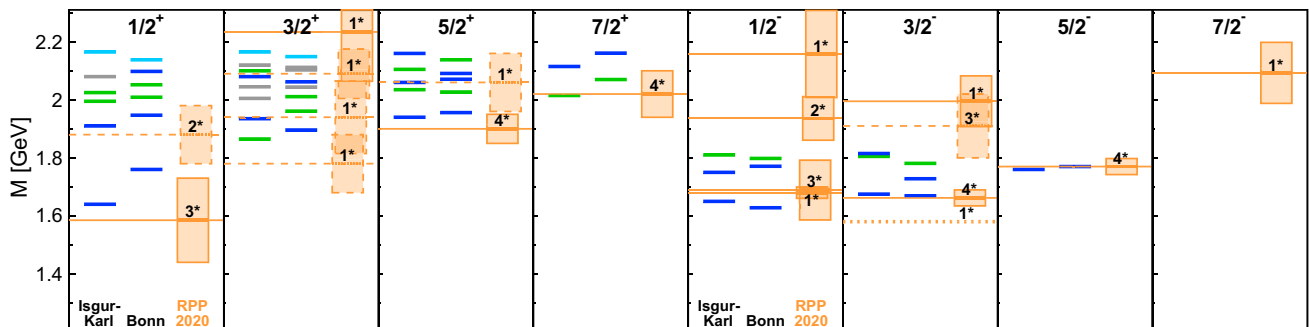


**Fig. 4**  $\Sigma^*$  states given in the RPP'2020 are compared to the quark-model states of the  $1\hbar\omega$  and  $2\hbar\omega$  band calculated by Isgur–Karl [16, 17] and within the Bonn model [27]. For explanations related to the RPP-states see Fig. 2. For the quark-model states, the colors indicate the

main configuration of the state, if one specific configuration reaches a value above 50%:  $^410[56]$ ,  $^210[70]$  (green),  $^28[56]$ ,  $^28[70]$ , or  $^48[70]$  (blue),  $^28[20]$ , none of the configuration reaches 50% (gray)

10 MeV only, and seem to be strongly mixed. The higher-mass state has a slightly larger octet component ( $^48[70]$ ), for the lower-mass state, the decomposition is not given in [16] but the decuplet component must prevail. In the Bonn model, the heavier state is the one with the larger decuplet component ( $^210[70]$ ). Experimentally, the two higher-mass

states with  $J^P = 1/2^-$  and  $J^P = 3/2^-$  are found at a much higher mass than expected. This might be caused by repelling forces of two strongly-mixed states having similar masses, or there could be two or several unresolved states which are described by one effective resonance. One  $\Sigma$  resonance with

**Table 6** SU(3) coupling constants for  $\Sigma^*$  decays and the SU(6) predictions

Decay mode	$8 \rightarrow 8 + 8$		$10 \rightarrow 8 + 8$	
$\Sigma \rightarrow N \bar{K}$	$\sqrt{2}(2\alpha - 1)A_8$		$-\sqrt{\frac{1}{6}}A_{10}$	
$\Sigma \rightarrow \Sigma \pi$	$2\sqrt{2} \cdot \alpha A_8$		$\sqrt{\frac{1}{6}}A_{10}$	
$\Sigma \rightarrow \Lambda \pi$	$-\frac{2}{\sqrt{3}}(\alpha - 1)A_8$		$-\frac{1}{2}A_{10}$	
	${}^28[56]$	${}^28[70]$	${}^48[70]$	${}^{2,4}[10]$
$\frac{A(\Sigma \rightarrow N \bar{K})}{A(\Sigma \rightarrow \Sigma \pi)}$	$-\frac{1}{4}$	$\frac{1}{5}$	2	-1
Sign	-	+	+	-
$\frac{A(\Sigma \rightarrow \Lambda \pi)}{A(\Sigma \rightarrow \Sigma \pi)}$	$\frac{1}{2}\sqrt{\frac{3}{2}}$	$\frac{1}{5}\sqrt{\frac{3}{2}}$	$-\sqrt{\frac{3}{2}}$	$-\sqrt{\frac{3}{2}}$
Sign	+	+	-	-

$J^P = 3/2^-$  expected in the first excitation shell, either in the  ${}^48[70]$  or in the  ${}^210[70]$  configuration, has not been found.

In the second excitation band, there is again one case—with  $J^P = 3/2^+$ —where a different level ordering is predicted in the two models. In the Bonn model, the lowest-mass state  $\Sigma(1780)3/2^+$  is in dominantly in the  ${}^28[56]$  multiplet and interpreted as the partner of  $\Sigma(1915)5/2^+$ . The  $\Sigma(1940)3/2^+$  is assigned to  ${}^410[56]$  and would be the state that corresponds to the Roper-like state  $\Delta(1600)3/2^+$ . The Isgur–Karl model sees  $\Sigma(1780)3/2^+$  as Roper-like state mainly in the  ${}^410[56]$  multiplet and  $\Sigma(1940)3/2^+$  in  ${}^28[56]$  and as spin partner of  $\Sigma(1915)5/2^+$ . We think the Isgur–Karl interpretation is more likely, in agreement with the lattice results [31]. Radial excitations are often predicted at too high masses in quark models; the Roper resonance  $N(1440)1/2^+$  is the best-known example.

The next states  $\Sigma(2080)3/2^+$  and  $\Sigma(2070)5/2^+$  could be members of a spin-quartet with  $\Sigma(2030)7/2^+$  as resonance with the largest total angular momentum, and could belong preferentially to the  ${}^410[56]$  multiplet. The two models are not in conflict with this interpretation even though the mixing of the  $\Sigma(2080)3/2^+$  resonance is strong in the Isgur–Karl model. These states correspond to  $\Delta(1920)3/2^+$ ,  $\Delta(1905)5/2^+$ ,  $\Delta(1950)7/2^+$  in the non-strange sector.

## 5.2 SU(3) constraints for $\Sigma^*$ decays

Table 6 lists the coupling constants for  $\Sigma$  resonances into  $N \bar{K}$ ,  $\Sigma \pi$ , and  $\Lambda \pi$ . The  $\alpha$  ratios for the different decay modes were given in Table 3. In Table 7 we compare the predicted phases with experimental values. The old analyses and the KSU analysis give clear answers to the phases: they are at  $0^\circ$  or at  $180^\circ$ . The Osaka-ANL and BnGa analysis give phases at any value. Here, we give numbers which range from  $-180^\circ$  to  $180^\circ$ .

In the low-energy region, Osaka-ANL and BnGa find phases that are incompatible with the expectation. Indeed,  $\Sigma(1620)1/2^-$  and  $\Sigma(1750)1/2^-$  were difficult to separate in the BnGa analysis, and Osaka-ANL finds only  $\Sigma(1620)1/2^-$  in model B and only  $\Sigma(1750)1/2^-$  in model A. Also  $\Sigma(1660)1/2^+$  does not show the expected phases, neither in the Osaka-ANL nor in the BnGa analysis. Due to its high spin at a low mass,  $\Sigma(1775)5/2^-$  can be identified rather well in partial-wave analyses. Its SU(3) structure can be deduced consistently from the partial-wave analyses (in the BnGa analysis, the relative phases are at least compatible with the expectations within  $3\sigma$ ).

In about 1800 MeV, a further spin doublet of states with  $J^P = 1/2^-$  and  $3/2^-$  is expected that would correspond to  $\Delta(1620)1/2^-$  and  $\Delta(1700)3/2^-$ . Two states are found, indeed, but at about 1900 MeV:  $\Sigma(1900)1/2^-$  and  $\Sigma(1910)3/2^-$ . The conflicting results on their SU(3) structure seem also not to be compatible with an assignment to a spin-doublet SU(3) decuplet. Likely, higher-mass resonances and these states are not separately identified.

The  $\Sigma(1915)5/2^+$  and  $\Sigma(2030)7/2^+$  resonances are both well established. Their phases are at least qualitatively compatible with their common interpretation as companion of  $N(1680)5/2^+$  and  $\Delta(1950)7/2^+$ .

The  $\Sigma(2100)7/2^-$  resonance might be the hyperon partner of  $N(2190)7/2^-$  even though its mass would rather be expected at a 200 MeV higher mass. Alternatively, it could belong to the  $(70, 2^-)$  multiplet. In both cases, the low mass is surprising.

## 6 Comparison of $\Lambda$ and $\Sigma$ spectrum with the $N$ and $\Delta$

Finally, we present in Table 8 a comparison of the spectrum of  $\Lambda$  and  $\Sigma$  resonances with those for  $N$  and  $\Delta$  resonances. Mostly, the masses of  $\Lambda$  and  $\Sigma$  resonances are 100–200 MeV higher than the masses of their  $N$  and  $\Delta$  counterparts. The SU(3) singlet states have, of course, no states in the  $N/\Delta$  sector to be compared with.

The  $\Lambda$  spectrum expected in the first excitation band is nearly complete, with a  $J^P = 3/2^-$   $\Lambda$  as missing particle. The  $\Lambda(1380)1/2^-$  and  $\Lambda(1405)1/2^-$  resonances are below the  $K^-p$  threshold and were not reported (except in Ref. [43], model B where it is seen with a mass of 1512 MeV and with a very large width). Based on their masses and phases, the other states are in most cases consistently identified as singlets or octet states.

The results on the  $\Sigma$  states in the first excitation shell are much less consistent. Here, the assignment of the four lowest-mass negative-parity states to the expected spin doublet and triplet is plausible when the masses are considered but not on the basis of their decays. Again, one  $3/2^-$  state is missing. The states  $\Sigma(1900)1/2^-$  and  $\Sigma(1910)3/2^-$

**Table 7** The phase differences  $\delta\phi$  between the amplitudes for  $K^- p \rightarrow \Sigma^* \rightarrow \Sigma\pi$  and  $K^- p \rightarrow \Sigma^* \rightarrow \bar{K}N / K^- p \rightarrow \Sigma^* \rightarrow \Lambda\pi$  and  $K^- p \rightarrow \Sigma^* \rightarrow \Sigma\pi$  on the real axis (2012, KSU) and at the  $\Sigma^*$  pole (Osaka-ANL and BnGa). 2012 stands for results listed in Ref. [6] when the results from different groups are mostly consistent. The relative sign

$\Sigma^*$	$\delta\phi$					
	Expected	2012	KSU	Osaka-ANL <sub>A</sub>	Osaka-ANL <sub>B</sub>	BnGa
$\Sigma(1620)1/2^-$	0/0°	0/0°	0/0°		−124/−45°	−(133±33)/(165±33)°
$\Sigma(1670)3/2^-$	0/0°	0/0°	0/0°	−57/162°	14/−31°	(6±16)/(−27±16)°
$\Sigma(1750)1/2^-$	0/180°		0/0°	−41/32°		−(116±23)/(15±23)°
$\Sigma(1775)5/2^-$	0/180°	0/180°	0/180°	8/−179°	−1/−174°	(27±16)/(120±19)°
$\Sigma(1900)1/2^-$	†	0/0°	0°/180° <sup>x</sup>		−3/−25°	(5±32)/(105±54)°
$\Sigma(1910)3/2^-$	†	180/0°				−(65±62)/(−175±29)°
$\Sigma(1660)1/2^+$	180/0°		180/0° <sup>x</sup>	−90/−162°	174/−50°	−(45±40)/(−150±32)°
$\Sigma(1880)1/2^+$	0/0°	0/180°	180/0° <sup>x</sup>			
$\Sigma(1780)3/2^+$	180/180°		0/0°			
$\Sigma(1940)3/2^+$	180/0°		0/0° <sup>x</sup>			
$\Sigma(1915)5/2^+$	180/0°	180/0°	180/0°	172/9°		−(147±19)/(10±23)°
$\Sigma(2080)3/2^+$	180/180°					
$\Sigma(2070)5/2^+$	180/180°	0°/−				
$\Sigma(2030)7/2^+$	180/180°	180/180°	180/180°	173/−159°	88/−87°	−(157±14)/(173±17)°
$\Sigma(2100)7/2^-$		0/180°	0/180°			(60±25)/(−50±32)°
$\Sigma(2110)1/2^-$	†		180/180° <sup>x</sup>			(15±49)/(90±43)°
$\Sigma(2010)3/2^-$	†					−(115±33)/(40±33)°

are considerably more massive than their possible partners  $\Delta(1620)1/2^-$  and  $\Delta(1700)3/2^-$ . Likely, the  $\Sigma(1900)1/2^-$  and  $\Sigma(1910)3/2^-$  structures contain more than one resonance each.

In the third excitation shell, partners of  $N(1895)1/2^-$ ,  $N(1875)3/2^-$ ,  $\Delta(1900)1/2^-$ ,  $\Delta(1940)3/2^-$ , and  $\Delta(1930)5/2^-$  are expected. Their masses are well separated from the states in the first excitation shell,  $\Delta(1620)1/2^-$  and  $\Delta(1700)3/2^-$ , which should be accompanied with  $\Sigma$  states at about 1800 MeV. The  $\Sigma$  partners of the  $N^*$  doublet should have masses above 2000 MeV, the partners of the  $\Delta$  triplet masses of about 2100 MeV. We observe a doublet,  $\Sigma(1900)1/2^-$  and  $\Sigma(1910)3/2^-$  instead of states at 1800 MeV and above 2000 MeV. When  $\Sigma(1900)1/2^-$  and  $\Sigma(1910)3/2^-$  are made of more than single resonances, a clear identification of their SU(6) structure cannot be expected. A further pair of states is seen:  $\Sigma(2110)1/2^-$  and  $\Sigma(2010)3/2^-$ . Thus we expect three states with  $J^P = 1/2^-$  and three with  $J^P = 3/2^-$  in the (approximate) mass range from 1800 to 2100 MeV. Two pairs are observed, a third pair and a  $J^P = 5/2^-$  state are missing. At present, it is not possible to decide which states are seen and which are not.

The four states  $\Lambda(1600)1/2^+$ ,  $\Lambda(1810)1/2^+$ ,  $\Sigma(1660)1/2^+$ ,  $\Sigma(1880)1/2^+$  are likely the SU(3) partner states of  $N(1440)1/2^+$  and  $N(1710)1/2^+$ .  $\Sigma(1780)3/2^+$  could be the hyperon candidate for a partner of  $\Delta(1600)3/2^+$ . Again,

or phase is not given in Ref. [44]. For the Osaka-ANL, the results from model A and B are quoted. A index <sup>x</sup> denotes entries with a nearly vanishing amplitude. The two doublets with a dagger † may have contributions from three SU(6) configurations (see Table 8). See text for which phases are to be “expected”

in some cases the decay modes are in conflict with these interpretations.

The spin doublets  $\Lambda(1890)3/2^+/\Lambda(1820)5/2^+$  and  $\Sigma(1915)5/2^+/\Sigma(1940)3/2^+$  are easily interpreted as the strange partners of  $N(1720)3/2^+/N(1680)5/2^+$ , this assignment follows from their masses, and is suggested in the Isgur–Karl model. Three of these states are listed with four stars, only  $\Sigma(1940)3/2^+$  is not (yet) established. For the three established states, the phases support this assignment. The Bonn model suggests  $\Sigma(1780)3/2^+$  to be the spin partner of  $\Sigma(1940)3/2^+$ . We prefer to identify  $\Sigma(1780)3/2^+$  as first decuplet radial excitation and hyperon partner of  $\Delta(1600)3/2^+$ .

The CLAS collaboration claimed a double structure in the region of  $N(1720)3/2^+$  [72, 73]. A combined fit to data on  $\pi^+\pi^-p$  photo- and electroproduction requires two states, the conventional  $N(1720)3/2^+$  state (shifted in mass to  $\approx 1750$  MeV), and a new state at  $\approx 1725$  MeV. This state could be a candidate for the  $(D, L_N^P) S J^P = (70, 2_2^+) \frac{1}{2} \frac{3}{2}^+$  slot.

The three states  $\Lambda(2070)3/2^+$ ,  $\Lambda(2110)5/2^+$ , and  $\Lambda(2085)7/2^+$  are close in mass and could be interpreted as quartet of states with internal quantum numbers  $L = 2$ ,  $S = 3/2$  with the  $J^P = 1/2^+$  state missing. In the case of  $\Lambda(2085)7/2^+$ , this interpretation is unambiguous. This is not the case for  $\Lambda(2070)3/2^+$  and  $\Lambda(2110)5/2^+$ . The Bonn model interprets the latter two states as spin doublet and assigns them to the

**Table 8** Comparison of the hyperon spectrum with  $N$  and  $\Delta$  excitations. In the first and second excitation band, all expected states are shown. The third band lists only bands for which at least one  $\Lambda$  or  $\Sigma$  candidate exists. The states with a dagger † are special: one pair is expected

at about 1750 to 1800 MeV, two pairs at about 2000–2050 MeV. Two pairs are found only. They are shown with two possible assignments. Likely, the two observed pairs of states are each mixtures of these three configurations. A third pair is missing

$(D, L_N^P) S J^P$	Singlet	Octet	Decuplet			
$(56, 0_0^+) \frac{1}{2} \frac{1}{2}^+$		$N(939)$	$\Lambda(1116)$	$\Sigma(1193)$		
$\frac{3}{2} \frac{3}{2}^+$					$\Delta(1232)$	$\Sigma(1385)$
$(70, 1_1^-) \frac{1}{2} \frac{1}{2}^-$	$\Lambda(1405)$	$N(1535)$	$\Lambda(1670)$	$\Sigma(1620)$	$\Delta(1620)$	$\Sigma(1900)^\dagger$
$\frac{3}{2}^-$	$\Lambda(1520)$	$N(1520)$	$\Lambda(1690)$	$\Sigma(1670)$	$\Delta(1700)$	$\Sigma(1910)^\dagger$
$\frac{3}{2} \frac{1}{2}^-$		$N(1650)$	$\Lambda(1800)$	$\Sigma(1750)$		
$\frac{3}{2}^-$		$N(1700)$	–	–		
$\frac{5}{2}^-$		$N(1675)$	$\Lambda(1830)$	$\Sigma(1775)$		
$(56, 0_2^+) \frac{1}{2} \frac{1}{2}^+$		$N(1440)$	$\Lambda(1600)$	$\Sigma(1660)$		
$\frac{3}{2} \frac{3}{2}^+$					$\Delta(1600)$	$\Sigma(1780)$
$(70, 0_2^+) \frac{1}{2} \frac{1}{2}^+$	$\Lambda(1710)$	$N(1710)$	$\Lambda(1810)$	$\Sigma(1880)$	$\Delta(1750)$	–
$\frac{3}{2} \frac{3}{2}^+$		–	–	–		
$(56, 2_2^+) \frac{1}{2} \frac{3}{2}^+$		$N(1720)$	$\Lambda(1890)$	$\Sigma(1940)$		
$\frac{1}{2} \frac{5}{2}^+$		$N(1680)$	$\Lambda(1820)$	$\Sigma(1915)$		
$\frac{3}{2} \frac{1}{2}^+$					$\Delta(1910)$	
$\frac{3}{2} \frac{3}{2}^+$					$\Delta(1920)$	$\Sigma(2080)$
$\frac{3}{2} \frac{5}{2}^+$					$\Delta(1905)$	$\Sigma(2070)$
$\frac{3}{2} \frac{7}{2}^+$					$\Delta(1950)$	$\Sigma(2030)$
$(70, 2_2^+) \frac{1}{2} \frac{3}{2}^+$	$\Lambda(2070)$		–	–	–	–
$\frac{5}{2}^+$	$\Lambda(2110)$	$N(1860)$	–	–	$\Delta(2000)$	–
$\frac{3}{2} \frac{1}{2}^+$		$N(1880)$	–	–		
$\frac{3}{2}^+$		$N(1900)$	–	–		
$\frac{5}{2}^+$		$N(2000)$	–	–		
$\frac{7}{2}^+$		$N(1990)$	$\Lambda(2085)$	–		
$(20, 1_2^+) \frac{1}{2} \frac{1}{2}^+$	–	–	–	–		
$\frac{3}{2}^+$	–	–	–	–		
$\frac{5}{2}^+$	–					
$(56, 1_3^-) \frac{1}{2} \frac{1}{2}^-$		$N(1895)$	$\Lambda(2000)$	$\Sigma(1900)^\dagger$		
$\frac{3}{2}^-$		$N(1875)$	$\Lambda(2050)$	$\Sigma(1910)^\dagger$		
$\frac{3}{2} \frac{1}{2}^-$					$\Delta(1900)$	$\Sigma(2110)^\dagger$
$\frac{3}{2}^-$					$\Delta(1940)$	$\Sigma(2010)^\dagger$
$\frac{5}{2}^-$					$\Delta(1930)$	–
$(70, 3_3^-) \frac{1}{2} \frac{5}{2}^-$	$\Lambda(2080)$	$N(2060)$	–	–	–	–
$\frac{7}{2}^-$	$\Lambda(2100)$	$N(2190)$	–	$\Sigma(2100)$	$\Delta(2200)$	–

$^2 1[70]$  SU(3) singlet. The decay modes from BnGa are compatible with this interpretation. In the Isgur–Karl model, the  $\Lambda(2070)3/2^+$  resonance is heavily mixed, but still the largest contribution stems from the  $^2 1[70]$  SU(3) singlet. For

$\Lambda(2110)5/2^+$ , both models—and the decay mode analysis—agree that this is a SU(3) singlet state.

The  $\Delta(1950)7/2^+$  resonance is prominently observed in  $\pi N$  induced reactions. This is the reason why we assign  $\Sigma(2030)7/2^+$  to the SU(3) decuplet, and this assignment



is mostly compatible with the decay mode analysis. There are two states,  $\Sigma(2080)3/2^+$ ,  $\Sigma(2070)5/2^+$ , that could be the spin partners of  $\Sigma(2030)7/2^+$ , with a  $J^P = 1/2^+$  state missing.

The states  $\Lambda(2000)1/2^-/\Lambda(2050)3/2^-$  and  $\Sigma(1900)1/2^-/\Sigma(2010)3/2^-$  may form two spin doublets and could fall, jointly with  $N(1895)1/2^-$  and  $N(1875)3/2^-$  and with  $\Delta(1900)1/2^-$ ,  $\Delta(1940)3/2^-$ ,  $\Delta(1930)5/2^-$  into the  $(56, 1_3^-)$  multiplet, with three missing  $\Sigma$  states, but this is speculative at the moment. The  $(56, 1_3^-)$  multiplet houses states that carry one unit of orbital angular momentum and one unit of radial excitation. It belongs to the third excitation band.

In comparison to the  $N$  and  $\Delta$  spectrum, there are still many empty slots, and many of the states in Table 8 are observed with weak evidence only. There is certainly need for new data. Indeed, new data on hyperon spectroscopy can be expected from J-PARC [65], JLAB [74], and the forthcoming PANDA experiment [75]. The combined analyses of both exclusive meson photo- and electroproduction data from JLab [76] offer a novel direction in the extension of our knowledge of the spectrum of the excited states of the nucleon. These studies might help to fill the vacant places in Table 8 and will guide the search for new  $\Lambda$  and  $\Sigma$  hyperons. Possibly, also existing (and forthcoming) data from JLab [15] and LHCb [77] can contribute to hyperon spectroscopy.

## 7 Summary

The spectrum of  $\Lambda$  and  $\Sigma$  excitations has been re-analyzed recently by four different groups. The analyses used different coupled-channel approaches; the resulting spectrum showed the same leading resonances, mostly 3-star and 4-star resonances in the RPP notation, and different sets of additional resonances. In this paper, we took into account hyperon resonances that were seen in one of the recent partial-wave analyses. The resulting spectrum was compared with the Isgur–Karl model and the Bonn model. The SU(3) structure of the observed resonances was discussed by comparison with the model calculations and by a comparison of the observed decay modes with SU(6) phase relations. In the  $\Lambda$  sector, there is reasonable agreement between the identification of singlet or octet states based on the comparison of observed states with the quark model and the identification based on the relative phases between decay modes. Seven  $\Lambda$  states are proposed to be classified as SU(3) singlet states. In the  $\Sigma$  sector, the identification of octet or decuplet states is consistent only for a few leading resonances. In both sectors, the first excitation shells are filled, except for the missing  $3/2^-$  states. However, several states are seen only with poor evidence. In the second shell, there are numerous missing states and queryPlease provide an explanation as to why there is no

data or why the data will not be deposited. Your explanation will be displayed as ‘Authors’ comment’.most states are not yet established. New data are certainly utterly needed. Nevertheless, the comparison of the resulting hyperon spectrum with the spectrum of  $N$  and  $\Delta$  resonances shows evidence for SU(3) symmetry. It is remarkable that even the  $1^*$  resonances find a slot in this comparison.

**Acknowledgements** This work was supported by the *Deutsche Forschungsgemeinschaft* (Bonn: SFB/TR110), the US Department of Energy grant DE-SC0016582, the JSA/ DOE Contract DE-AC05-06OR23177, and the *Russian Science Foundation* (RSF 16-12-10267). We thank J. Kohlen for drawing the figures.

**Funding** Open Access funding enabled and organized by Projekt DEAL.

**Data Availability Statement** This manuscript has no associated data or the data will not be deposited. [Authors’ comment: The data are available in the Review of Particle Properties. P.A. Zyla et al. [Particle Data Group], Review of Particle Physics, PTEP **2020**(8), 083C01 (2020).]

**Open Access** This article is licensed under a Creative Commons Attribution 4.0 International License, which permits use, sharing, adaptation, distribution and reproduction in any medium or format, as long as you give appropriate credit to the original author(s) and the source, provide a link to the Creative Commons licence, and indicate if changes were made. The images or other third party material in this article are included in the article’s Creative Commons licence, unless indicated otherwise in a credit line to the material. If material is not included in the article’s Creative Commons licence and your intended use is not permitted by statutory regulation or exceeds the permitted use, you will need to obtain permission directly from the copyright holder. To view a copy of this licence, visit <http://creativecommons.org/licenses/by/4.0/>.

## References

1. D.G. Ireland, E. Pasyuk, I. Strakovsky, Prog. Part. Nucl. Phys. **111**, 103752 (2020)
2. V. Crede, W. Roberts, Rept. Prog. Phys. **76**, 076301 (2013)
3. E. Klempt, J.M. Richard, Rev. Mod. Phys. **82**, 1095–1153 (2010)
4. I.G. Aznauryan, V.D. Burkert, Prog. Part. Nucl. Phys. **67**, 1–54 (2012)
5. D.S. Carman, K. Joo, V.I. Mokeev, Few Body Syst. **61**(3), 29 (2020)
6. J. Beringer et al., Particle data group. Phys. Rev. D **86**, 010001 (2012)
7. A. Starostin et al., [Crystal Ball Collaboration]. Phys. Rev. C **64**, 055205 (2001)
8. S. Prakhov et al., Phys. Rev. C **69**, 042202 (2004)
9. S. Prakhov et al., Phys. Rev. C **70**, 034605 (2004)
10. R. Manweiler et al., Phys. Rev. C **77**, 015205 (2008)
11. S. Prakhov et al., Phys. Rev. C **80**, 025204 (2009)
12. K. Moriya et al., [CLAS Collaboration]. Phys. Rev. Lett. **112**, 082004 (2014)
13. K. Moriya et al. [CLAS], Phys. Rev. C **87**(3), 035206 (2013)
14. H. Lu et al., [CLAS]. Phys. Rev. C **88**, 045202 (2013)
15. K. Moriya et al. [CLAS Collaboration], Phys. Rev. C **88**, 045201 (2013). Addendum: [Phys. Rev. C **88**, 049902 (2013)]
16. N. Isgur, G. Karl, Phys. Rev. D **18**, 4187 (1978)
17. N. Isgur, G. Karl, Phys. Rev. D **19**, 2653 (1979). Erratum: [Phys. Rev. D **23**, 817 (1981)]

18. S. Capstick, N. Isgur, Phys. Rev. D **34**, 2809 (1986)
19. L.Y. Glozman, D.O. Riska, Phys. Rept. **268**, 263 (1996)
20. L.Y. Glozman, W. Plessas, K. Varga, R.F. Wagenbrunn, Phys. Rev. D **58**, 094030 (1998)
21. T. Melde, W. Plessas, B. Sengl, Phys. Rev. D **77**, 114002 (2008)
22. J. Ferretti, A. Vassallo, E. Santopinto, Phys. Rev. C **83**, 065204 (2011)
23. E. Santopinto, J. Ferretti, Phys. Rev. C **92**(2), 025202 (2015)
24. E. Santopinto, J. Ferretti, Few Body Syst. **57**(11), 1095–1101 (2016)
25. M.M. Giannini, E. Santopinto, Chin. J. Phys. **53**, 020301 (2015)
26. R.N. Faustov, V.O. Galkin, Phys. Rev. D **92**(5), 054005 (2015)
27. U. Löring, B.C. Metsch, H.R. Petry, Eur. Phys. J. A **10**, 447 (2001)
28. U. Löring, K. Kretzschmar, B.C. Metsch, H.R. Petry, Eur. Phys. J. A **10**, 309 (2001)
29. U. Löring, B.C. Metsch, H.R. Petry, Eur. Phys. J. A **10**, 395 (2001)
30. R.G. Edwards, J.J. Dudek, D.G. Richards, S.J. Wallace, Phys. Rev. D **84**, 074508 (2011)
31. R.G. Edwards et al. [Hadron Spectrum Collaboration], Phys. Rev. D **87**(5), 054506 (2013)
32. S.X. Qin, C.D. Roberts, S.M. Schmidt, Few Body Syst. **60**(2), 26 (2019)
33. C. Chen, G.I. Krein, C.D. Roberts, S.M. Schmidt, J. Segovia, Phys. Rev. D **100**(5), 054009 (2019)
34. N. Kaiser, T. Waas, W. Weise, Nucl. Phys. A **612**, 297 (1997)
35. J.A. Oller, U.-G. Meißner, Phys. Lett. B **500**, 263 (2001)
36. D. Jido, J.A. Oller, E. Oset, A. Ramos, U.-G. Meißner, Nucl. Phys. A **725**, 181 (2003)
37. A. Cieply, M. Mai, U.-G. Meißner, J. Smejkal, Nucl. Phys. A **954**, 17 (2016)
38. A.V. Anisovich, A.V. Sarantsev, V.A. Nikonov, V. Burkert, R. Schumacher, E. Klempt, “Hyperon III:  $K^-p - \pi \Sigma$  coupled-channel dynamics in the  $\Lambda(1405)$  mass region” accepted for publication in EPJA
39. U.-G. Meissner, Symmetry **12**, 981 (2020)
40. H. Zhang, J. Tulpan, M. Shrestha, D.M. Manley, Phys. Rev. C **88**(3), 035204 (2013)
41. H. Zhang, J. Tulpan, M. Shrestha, D.M. Manley, Phys. Rev. C **88**(3), 035205 (2013)
42. H. Kamano, S.X. Nakamura, T.-S.H. Lee, T. Sato, Phys. Rev. C **90**(6), 065204 (2014)
43. H. Kamano, S.X. Nakamura, T.-S.H. Lee, T. Sato, Phys. Rev. C **92**(2), 025205 (2015) Erratum: [Phys. Rev. C **95**, no. 4, 049903 (2017)]
44. C. Fernandez-Ramirez, I.V. Danilkin, D.M. Manley, V. Mathieu, A.P. Szczepaniak, Phys. Rev. D **93**(3), 034029 (2016)
45. M. Matveev, A.V. Sarantsev, V.A. Nikonov, A.V. Anisovich, U. Thoma, E. Klempt, Eur. Phys. J. A **55**(10), 179 (2019)
46. A.V. Sarantsev, M. Matveev, V.A. Nikonov, A.V. Anisovich, U. Thoma, E. Klempt, Eur. Phys. J. A **55**(10), 180 (2019)
47. A. Barbaro-Galtieri et al., “Table of particle properties - Particle Data Group,” In: Philadelphia 1970 conference, experimental meson spectroscopy, New York 1970, p. 655–664
48. A. Brandstetter et al., Nucl. Phys. B **39**, 13 (1972)
49. W. Cameron et al., [Rutherford-London Collaboration]. Nucl. Phys. B **146**, 327 (1978)
50. P.J. Litchfield, Phys. Lett. B **51**, (1974)
51. J. Olmsted et al., [Crystal Ball Collaboration]. Phys. Lett. B **588**, 29 (2004)
52. D.F. Kane, Phys. Rev. D **5**, 1583 (1972)
53. G. L. Kane, “Quasi Two-Body Reactions and Properties of Resonances,” UM-HE-74-3, LBL, unpublished note
54. P. Baillon, P.J. Litchfield, Nucl. Phys. B **94**, 39 (1975)
55. G.P. Gopal et al., [Rutherford-London Collaboration]. Nucl. Phys. B **119**, 362 (1977)
56. G.P. Gopal, “ $S = -1$  Baryons: An Experimental Review,” In: Proceedings of the 4th International Conference on Baryon Resonances (BARYON 1980), 14–16 July 1980. Toronto, Ontario, Canada. Edited by Nathan Isgur. 1980. 479p. Toronto, Canada, Univ. of Toronto, 1980. p 479
57. M. Tanabashi et al. [Particle Data Group], Phys. Rev. D **98**(3), 030001 (2018)
58. N.P. Samios, M. Goldberg, B.T. Meadows, Rev. Mod. Phys. **46**, 49 (1974)
59. V. Guzey, M.V. Polyakov, Ann. Phys. **13**, 673 (2004)
60. V. Guzey, M.V. Polyakov, SU(3) systematization of baryons. [arXiv:hep-ph/0512355](https://arxiv.org/abs/hep-ph/0512355) [hep-ph]
61. See Section 99.2 in Ref. [57]
62. R.D. Tripp, R.O. Bangerter, A. Barbaro-Galtieri, T.S. Mast, Phys. Rev. Lett. **21**, 1721 (1968)
63. S. Capstick, W. Roberts, Prog. Part. Nucl. Phys. **45**, S241–S331 (2000)
64. M. De Sanctis et al., Few Body Syst. **57**(12), 1177–1184 (2016)
65. K.H. Hicks, H. Sako, P45: 3-Body Hadronic Reactions for New Aspects of Baryon Spectroscopy. Proposal for J-PARC **E45**, (2013)
66. O. Krehl, C. Hanhart, S. Krewald, J. Speth, Phys. Rev. C **62**, 025207 (2000)
67. M. Mai, P. C. Bruns, U. G. Meissner, framework,” Phys. Rev. D **86**, 094033 (2012)]
68. M. Doring, E. Oset, D. Strottman, Induced reactions. Phys. Lett. B **639**, 59–67 (2006)
69. M. F. M. Lutz, E. E. Kolomeitsev, scattering,” Nucl. Phys. A **700**, 193–308 (2002)]
70. V.D. Burkert, C.D. Roberts, Rev. Mod. Phys. **91**(1), 011003 (2019)
71. C. Fernandez-Ramirez, I.V. Danilkin, V. Mathieu, A.P. Szczepaniak, Phys. Rev. D **93**(7), 074015 (2016)
72. E. Golovatch et al., [CLAS] Collaboration. Phys. Lett. B **788**, 371–379 (2019)
73. V.I. Mokeev et al., Phys. Lett. B **805**, 135457 (2020)
74. S. Adhikari et al., “Strange Hadron Spectroscopy with a Secondary  $K_L$  Beam at GlueX”, Proposal for JLAB PAC47 (2019)
75. F. Iazzi [PANDA Collaboration], AIP Conf. Proc. **1743**, 050006 (2016)
76. S. J. Brodsky et al., Int. J. Mod. Phys. E (in print)
77. R. Aaij et al., [LHCb Collaboration]. Phys. Rev. Lett. **115**, 072001 (2015)